

# Identify Critical KV Cache in LLM Inference from an Output Perturbation Perspective

Yuan Feng<sup>1,3†</sup> Junlin Lv<sup>1,3†</sup> Yukun Cao<sup>1,3</sup> Xike Xie<sup>2,3\*</sup> S. Kevin Zhou<sup>2,3</sup>

<sup>1</sup>School of Computer Science, University of Science and Technology of China (USTC), China

<sup>2</sup>School of Biomedical Engineering, USTC, China

<sup>3</sup>Data Darkness Lab, MIRACLE Center, Suzhou Institute for Advanced Research, USTC, China  
{yfung,junlinlv,ykcho}@mail.ustc.edu.cn, xkxie@ustc.edu.cn, s.kevin.zhou@gmail.com

## Abstract

Large language models have revolutionized natural language processing but face significant challenges of high storage and runtime costs, due to the transformer architecture’s reliance on self-attention, particularly the large Key-Value (KV) cache for long-sequence inference. Recent efforts to reduce KV cache size by pruning less critical entries based on attention weights remain empirical and lack formal grounding. This paper presents a formal study on identifying critical KV cache entries by analyzing attention output perturbation. Our analysis reveals that, beyond attention weights, the value states within KV entries and pretrained parameter matrices are also crucial. Based on this, we propose a perturbation-constrained selection algorithm that optimizes the worst-case output perturbation to identify critical entries. Evaluations on the Needle-in-a-Haystack test and Longbench benchmark show our algorithm enhances state-of-the-art cache eviction methods. Further empirical analysis confirms that our algorithm achieves lower output perturbations in over 92% attention heads in Llama model, thereby providing a significant improvement over existing methods.

## 1. Introduction

Autoregressive large language models (LLMs) using transformer architecture have excelled in tasks, like dialogue systems (Yi et al., 2024), chatbots (Achiam et al., 2023), intelligent agents (Wang et al., 2024), and code generation (Gu, 2023). However, the quadratic computational cost inherent in the transformer’s self-attention mechanism poses significant challenges for practical deployment. To mitigate this, LLMs often use a Key-Value (KV) cache, which stores intermediate results from the self-attention mechanism. Each KV cache entry corresponds to the KV states

of a past token, thus allowing for the bypassing of recomputation of these tokens during autoregressive generation. However, as sequence lengths increase, the number of KV cache entries expands dramatically. This expansion not only leads to considerable GPU memory overhead but also significantly increases I/O latency, hindering the deployment in real-world applications (Sun et al., 2024a).

Recent research has identified that only a subset of KV cache entries substantially contribute to the output of the self-attention mechanism (Zhang et al., 2024b; Liu et al., 2024a; Tang et al., 2024a). As a result, many methods, known as *cache eviction*, have been developed to reduce the KV cache size to fit within a given budget by evicting non-critical entries during inference. These methods effectively save GPU memory and improve subsequent decoding speed. Notably, H2O (Zhang et al., 2024b) and Scissorhands (Liu et al., 2024a) observe a power-law distribution of attention weights: a small fraction of KV cache entries consistently dominates the majority of attention weights, aligning closely with the concept of cache entry criticality during inference. These methods introduce frameworks that leverage accumulated attention weights to identify and preserve critical cache entries. Building on this, subsequent works (Adnan et al., 2024; Li et al., 2024; Feng et al., 2024) have refined attention weight accumulation and added operations like pooling and budget allocation to better preserve key information. However, while these methods generally assume that entries with higher attention weights—determined by the similarity between key states in the KV cache and the target query state—are critical, the identification and characterization of “critical cache entries” remain unformalized.

This assumption raises two key questions:

1. *What criteria determine the critical KV cache?*
2. *Is reliance on attention weights alone sufficient for identifying critical cache entries?*

In this paper, we define the problem of critical cache identification from the perspective of output perturbation and introduce a theoretical framework to bound the worst-case scenario for optimizing practical perturbation. Specifically,

<sup>†</sup>Equal Contribution <sup>\*</sup>Corresponding Author

we focus on minimizing attention output perturbation when replacing the full KV cache with only critical entries under a given budget. To quantify this perturbation, we employ the simple  $L_1$  distance and derive its upper bound<sup>1</sup>, corresponding to the worst-case perturbation. Our analysis shows that this upper bound is influenced by both the attention weights and the value states projected through the parameter matrix. Based on these insights, we propose a perturbation-constrained selection algorithm that goes beyond mere reliance on attention weights, underscoring the significance of previously overlooked value states and pre-trained parameter matrix in identifying critical cache entries.

We integrate our algorithm into two state-of-the-art (SOTA) cache eviction methods, SnapKV (Li et al., 2024) and AdaKV (Feng et al., 2024), replacing their reliance on solely attention-weight-based strategies. Through extensive evaluations using Needle-in-a-Haystack tests and 16 datasets from LongBench across two compression scenarios, our algorithm more accurately selects critical cache entries, significantly enhancing post-eviction generation quality under various budget constraints. Further empirical analysis confirms and elucidates the practical benefits of our algorithm: (1) It effectively reduces output perturbation in most attention heads, achieving over 92% heads in the Llama model. (2) Its advantages accumulate across layers, significantly lowering the perturbation in final-layer hidden states. (3) It consistently performs well across various cache sizes, robustly mitigating quality loss under different resource constraints in practical applications. Our contributions can be summarized as follows:

1. We highlight that current cache eviction methods neglect the crucial problem of identifying critical KV cache entries. To address this, we propose using output perturbation as a criterion for determining criticality. Our analysis shows that attention weights alone are insufficient; the value states projected by the parameter matrix are also essential.
2. Building on the constraint of the worst-case output perturbation, we propose a novel critical entry selection algorithm. When integrated into SOTA eviction methods, comprehensive evaluations across the Needle-in-a-Haystack test and Longbench benchmark demonstrate its effectiveness in improving generation quality.
3. Further empirical analysis examines and confirms the benefits of our perturbation-constrained selection algorithm. This analysis also highlights the significant potential for optimizing critical cache selection from the theoretical perspective of output perturbation.

<sup>1</sup>We choose the  $L_1$  distance due to its simplicity and effectiveness. More complex metrics, such as the  $L_2$  distance, are equally valid; see Appendix F for related discussions.

## 2. Related Works

**Perturbation-based analysis** has achieved remarkable success in neural network interpretability and pruning. For example, Catformer (Davis et al., 2021) and Admin (Liu et al., 2020) utilize output perturbation analysis to create more stable network architectures and enhance training methods. Similarly, pruning techniques (Han et al., 2015; Frantar & Alistarh, 2023), with Wanda (Sun et al., 2024b) as a representative, aim to identify neurons whose removal minimally impacts output, thereby reducing network parameters. In this paper, we present the first analysis of output perturbations aimed at developing more effective selection metrics for cache eviction in efficient LLM inference.

**KV cache eviction** aims to retain only critical KV cache entries while evicting non-essential ones to reduce cache size, facilitating efficient long-sequence inference in LLMs. Early methods (Xiao et al., 2023), which preserved recent entries in a sliding window, risked losing important information in long sequences. Techniques like H2O (Zhang et al., 2024b) and Scissorhands (Liu et al., 2024a) used accumulated attention scores to identify key entries, aiming to retain crucial context. Subsequent works refined these methods (Ge et al., 2024b; Adnan et al., 2024; Ge et al., 2024a; Li et al., 2024), with SnapKV (Li et al., 2024) achieving the SOTA performance through introducing observation window-based attention weight accumulation and pooling operations. Recent budget allocation optimization methods (Yang et al., 2024; Zhang et al., 2024a), exemplified by AdaKV (Feng et al., 2024), enhance post-eviction generation by allocating budgets based on attention head characteristics. However, these methods are largely empirical, relying solely on attention weights to identify critical entries. Our paper introduces a novel perturbation-constrained selection algorithm based on in-depth analysis from an output perturbation perspective. This algorithm seamlessly integrates into existing cache eviction methods without altering underlying accumulation processes. In our work, we demonstrate its effectiveness by applying it to SnapKV and AdaKV, all showing consistent improvements in post-eviction generation quality under varying budgets.

## 3. Critical KV Cache Entry Selection

For critical cache entry selection, we aim to choose cache entries that effectively represent the entire KV cache during self-attention computation, producing an output that is a close approximation, if not identical. Preliminaries about the relationship between KV cache and generation output are introduced in Section 3.1. Based on that, we formalize the problem of identifying critical cache entries from the perspective of output perturbation (Definition 3.1) in Section 3.2. Subsequently, in Section 3.3, we formalize the output perturbation and derive its upper bound. Then,

we propose a two-stage greedy algorithm in Section 3.4 that constrains worst-case perturbations for selecting critical entries, with theoretical analysis provided in Section 3.5. Finally, in Section 3.6 we integrate the algorithm into current SOTA cache eviction methods.

### 3.1. Preliminaries

LLMs utilizing the multi-head self-attention mechanism operate with an autoregressive generation approach. In this setup, each decoding step leverages the most recently generated token to predict the next one. To illustrate this process, we focus on a single attention head as an example. Let  $X \in \mathbb{R}^{n \times d}$  denote the embedding matrix for all tokens in the sequence, with  $x = X_{-1,:} \in \mathbb{R}^{1 \times d}$  representing the embedding vector of the most recent token, which serves as input at the current time step. The parameter matrices, denoted by  $W^Q$ ,  $W^K$ , and  $W^V \in \mathbb{R}^{d \times d_h}$  are used to map the token embeddings into their respective Query, Key, and Value states with head dimension  $d_h$  as follows:

$$q = xW^Q; K = XW^K; V = XW^V \quad (1)$$

During the decoding phase, the Key and Value states of previously generated tokens (represented by  $X$ ) are stored in the KV cache, allowing for the elimination of redundant computation. Accordingly, the query  $q$ , derived from the most recent token  $x$ , attends to the cached Key  $K$  to compute the attention weights  $A$ . These weights are then applied to the cached Value  $V$ , producing an intermediate output. This intermediate result is subsequently transformed into the final output  $o$  of the self-attention mechanism by the output parameter matrix  $W^O \in \mathbb{R}^{d_h \times d}$ :

$$o = AVW^O, \text{ where } A = \text{softmax}\left(qK^T/\sqrt{d}\right) \quad (2)$$

### 3.2. What criteria determine the critical KV cache?

Recent research has demonstrated only a small portion of critical KV cache entries do substantially contribute to the attention output (Zhang et al., 2024b; Liu et al., 2024a). This insight presents promising opportunities to reduce inference costs by evicting a large number of non-critical KV cache entries (Li et al., 2024; Zhang et al., 2024a; Feng et al., 2024; Ge et al., 2024b; Adnan et al., 2024; Ge et al., 2024a). However, the key challenge lies in accurately identifying the critical KV cache entries. Ideally, from a high-level perspective, the set of critical KV cache entries should completely represent the entire cache, ensuring for given query state, the selected entries yield the same attention output as the full set of KV pairs. In practice, the number of selected critical cache entries will be constrained by a predefined budget, which is closely tied to the computational resources available in downstream deployments. Consequently, our goal

shifts toward minimizing the output perturbation introduced by the replacement. So, the problem can be reformulated as follows.

**Definition 3.1** (Critical KV Cache Identification Problem). Given a critical cache budget  $b$ , the task is to select  $b$  critical KV cache entries  $\langle \hat{K}, \hat{V} \rangle$  from a total of  $n$  cache entries  $\langle K, V \rangle$ , with the goal of minimizing the perturbation in the attention output  $o$ . By using the  $L_1$  distance  $\mathcal{L}$  for quantification, the objective is formalized as:

$$\arg \min_{\text{selection of } \langle \hat{K}, \hat{V} \rangle} \mathcal{L} = \|o - \hat{o}\|_1 \quad (3)$$

where  $\hat{o}$  represents the attention output produced by the selected  $\langle \hat{K}, \hat{V} \rangle$ .

### 3.3. Are attention weights sufficient for identifying critical cache entries?

According to Definition 3.1, the goal of identifying critical KV cache entries is to minimize the perturbation  $\mathcal{L} = \|o - \hat{o}\|_1$ . To achieve this, we can employ an additive masking  $\mathcal{M}$  to simulate the removal of non-critical cache entries' contributions to the final output  $\hat{o}$ , thereby altering  $\hat{o}$ .

$$\hat{o} = A'VW^O, \quad A' = \text{softmax}\left(\mathcal{M} + qK^T/\sqrt{d}\right) \quad (4)$$

$$\text{where } \mathcal{M}_i = \begin{cases} -\infty & \text{if } K_i \text{ and } V_i \text{ are non-critical} \\ 0 & \text{otherwise.} \end{cases}$$

Thus, the perturbation  $\mathcal{L}$  can be further expressed as:

$$\mathcal{L} = \|(A - A')VW^O\|_1 \quad (5)$$

**Theorem 3.2.** By introducing a mask  $\mathcal{N} \in \mathbb{R}^n$  applied through element-wise multiplication denoted by  $\odot$ , we can establish the relation between  $A'$  and  $A$  as follows:

$$A' = \frac{\mathcal{N} \odot A}{\sum_{i=1}^n \mathcal{N}_i A_i} \quad (6)$$

$$\text{where } \mathcal{N}_i = \begin{cases} 0 & \text{if } K_i, V_i \text{ is non-critical} \\ 1 & \text{otherwise.} \end{cases} \text{ and } \sum_{i=1}^n \mathcal{N}_i = b$$

*Proof.* Let  $a = qK^T/\sqrt{d}$ , we can express the attention weights  $A'$  under critical cache entries as:

$$\begin{aligned} A' &= \frac{\exp(\mathcal{M} + a)}{\sum_{i=1}^n \exp(\mathcal{M} + a)_i} \\ &= \frac{\mathcal{N} \odot \exp(a)}{\sum_{i=1}^n \mathcal{N}_i \exp(a)_i} \\ &= \mathcal{N} \odot \frac{\exp(a)}{\sum_{i=1}^n \exp(a)_i} \frac{\sum_{i=1}^n \exp(a)_i}{\sum_{i=1}^n \mathcal{N}_i \exp(a)_i} \end{aligned} \quad (7)$$

Considering  $A = \frac{\exp(a)}{\sum_{i=1}^n \exp(a)_i}$ , thus  $\sum_{i=1}^n \mathcal{N}_i A_i = \frac{\sum_{i=1}^n \mathcal{N}_i \exp(a)_i}{\sum_{i=1}^n \exp(a)_i}$ . Therefore,  $A' = \frac{\mathcal{N} \odot A}{\sum_{i=1}^n \mathcal{N}_i A_i}$ .  $\square$

Theorem 3.2 utilizes a multiplicative mask  $\mathcal{N}$  to quantifies how their selection impacts the attention weights. However, directly minimizing  $\mathcal{L}$  for critical cache selection is challenging due to complex matrix operations it requires. Thus we turn to establish an upper bound  $\theta$ , as shown in Theorem 3.3.

**Theorem 3.3.** *The output perturbation  $\mathcal{L}$  can be bounded by  $\theta$ :*

$$\mathcal{L} \leq \theta = C - \left(2 - \frac{1}{\sum_{i=1}^n \mathcal{N}_i A_i}\right) \sum_{i=1}^n \mathcal{N}_i A_i \|\mathbf{v}_{i,:}\|_1, \quad (8)$$

where  $C$  denotes the  $\sum_{i=1}^n A_i \|\mathbf{v}_{i,:}\|_1$  and  $\mathbf{V} \in \mathbb{R}^{n \times d} = VW^O$  denotes all projected values states through parameter matrix  $W^O$ .

*Proof.* Let  $\mathbf{V} \in \mathbb{R}^{n \times d} = VW^O$  denote all projected value states, thus:

$$\mathcal{L} = \left\| \left( A - \frac{\mathcal{N} \odot A}{\sum_{i=1}^n \mathcal{N}_i A_i} \right) \mathbf{V} \right\|_1 \quad (9)$$

$$\begin{aligned} &= \left\| \sum_{i=1}^n \left( A_i - \frac{\mathcal{N}_i A_i}{\sum_{i=1}^n \mathcal{N}_i A_i} \right) \mathbf{v}_{i,:} \right\|_1 \\ &\leq \theta = \sum_{i=1}^n \left\| \left( A_i - \frac{\mathcal{N}_i A_i}{\sum_{i=1}^n \mathcal{N}_i A_i} \right) \mathbf{v}_{i,:} \right\|_1 \quad (10) \\ &= \sum_{i=1}^n \left| A_i - \frac{\mathcal{N}_i A_i}{\sum_{i=1}^n \mathcal{N}_i A_i} \right| \times \|\mathbf{v}_{i,:}\|_1 \end{aligned}$$

Given that the multiplicative mask  $\mathcal{N}$  is either 0 or 1, the index set  $i \in [1, n]$  can be split into  $I_0$  and  $I_1$ , according to its value. Thus:

$$\theta = \sum_{i \in I_0} A_i \|\mathbf{v}_{i,:}\|_1 + \sum_{i \in I_1} \left( \frac{A_i}{\sum_{i=1}^n \mathcal{N}_i A_i} - A_i \right) \|\mathbf{v}_{i,:}\|_1 \quad (11)$$

Let  $C$  represent  $\sum_{i=1}^n A_i \|\mathbf{v}_{i,:}\|_1$ , a constant independent of the selection of critical entries. We can express  $\sum_{i \in I_0} A_i \|\mathbf{v}_{i,:}\|_1$  as  $C - \sum_{i \in I_1} A_i \|\mathbf{v}_{i,:}\|_1$ . Thus:

$$\begin{aligned} \mathcal{L} &\leq \theta = C + \sum_{i \in I_1} \left( \frac{A_i}{\sum_{i=1}^n \mathcal{N}_i A_i} - 2A_i \right) \|\mathbf{v}_{i,:}\|_1 \quad (12) \\ &= C - \left( 2 - \frac{1}{\sum_{i=1}^n \mathcal{N}_i A_i} \right) \sum_{i=1}^n \mathcal{N}_i A_i \|\mathbf{v}_{i,:}\|_1 \end{aligned}$$

$\square$

We can observe that  $\theta$  encompasses not only the attention weights but also the projected value states. This highlights that prior selection methods relying solely on attention weights are suboptimal.

#### Algorithm 1 Perturbation-Constrained Selection

**Input:** Budgets  $b$ , Query State  $q$ , KV Cache Entries  $K, V$ , Parameter Matrix  $W^O$ , Hyper Parameter  $\alpha = 0.25$

**Output:** Critical Cache Entries  $\hat{K}, \hat{V}$

```

1: initialize empty cache  $\hat{K}, \hat{V}$ 
2:  $A = \text{softmax}(qK^T)$ ;  $\mathbf{V} = VW^O$ 
3:  $\mathcal{A} = (A + \epsilon) \odot (L_1 \text{ norm of each rows in } \mathbf{V})$ 
4:  $b' = b \times \alpha$ ;  $b'' = b - b'$ 
5: for  $A_i, K_i, V_i \in A, K, V$  do                                Start of Stage 1
6:   if  $A_i \in \text{Top}_k(A, b')$  then
7:     add  $K_i, V_i$  to  $\hat{K}, \hat{V}$ 
8:     remove  $\mathcal{A}_i, K_i, V_i$  from  $\mathcal{A}, K, V$ 
9:   end if
10: endfor                                                            End of Stage 1
11: for  $\mathcal{A}_i, K_i, V_i \in \mathcal{A}, K, V$  do                                Start of Stage 2
12:   if  $\mathcal{A}_i \in \text{Top}_k(\mathcal{A}, b'')$  then
13:     add  $K_i, V_i$  to  $\hat{K}, \hat{V}$ 
14:   end if
15: endfor                                                            End of Stage 2
return Critical Cache Entries  $\hat{K}, \hat{V}$ 

```

#### 3.4. Identify critical cache entries by constraining worst-case perturbation.

Drawing on optimization strategies in machine learning, we propose lowering the upper bound of perturbation, effectively constraining the worst-case perturbation and thereby reducing actual perturbations for identifying critical cache entries. However, directly minimizing the upper bound  $\theta$  remains non-trivial. To balance both the complexity and selection effectiveness, we introduce a two-stage greedy perturbation-constrained selection Algorithm 1, specifically designed to lower the perturbation upper bound for critical cache entry identification.

In this algorithm, the total budget  $b$  is divided into two portions based on a hyperparameter  $\alpha$ . In the first stage, a fraction of the budget,  $b' = b \times \alpha$ , is allocated to prioritize KV cache entries with high attention weights. In the second stage, the remaining budget,  $b'' = b - b'$ , is used to consider both the norms of the projected value states and the attention weights<sup>2</sup>. This two-stage selection employs a Top-K operation to effectively constrain the worst-case perturbation. To substantiate the effectiveness of our proposed algorithm, we provide a theoretical analysis in the following section.

#### 3.5. Theoretical analysis of Algorithm 1

Our proposed algorithm consists of two stages, referred to as stage 1 and stage 2, which work collaboratively to select critical cache entries. Under the guarantee provided by Assumption 3.4, the selection in stage 1 ensures that stage 2 adheres to the constraints on perturbations, as formalized in Theorem 3.5. Let  $\mathcal{N}'$  and  $\mathcal{N}''$  represent the selections from

<sup>2</sup>A small constant  $\epsilon$  (e.g., 1E-4) is added to attention weights to ensure numerical stability.

the stage 1 and 2, respectively, satisfying:  $\sum_{i=1}^n \mathcal{N}'_i = b'$  and  $\sum_{i=1}^n \mathcal{N}''_i = b''$ . Thus, the overall selection is  $\mathcal{N} = \mathcal{N}' + \mathcal{N}''$ .

**Assumption 3.4.** In the first stage, a portion of the overall budget  $b' = b \times \alpha$  is sufficient to collect the cache entries corresponding to the highest attention weights, ensuring their cumulative attention weights  $\sigma$  exceed half of the total, i.e.,  $\sigma = \sum_{i=1}^n \mathcal{N}'_i A_i = \sum \text{Top}_k(A, b') > 0.5$ .

In this paper, we set  $\alpha$  in Assumption 3.4 to a fixed value 0.5 based on two key considerations. First, as verified in Appendix A, allocating 50% of the total budget is sufficient to capture enough attention weight in over 99% of attention heads, thereby satisfying Assumption 3.4 across various settings. This is attributed to the power-law distribution of attention weights (Zhang et al., 2024b), where a small fraction of cache entries accounts for the majority of the weights. Second, this choice is both robust and easy to apply across different cache budgets and models. While using different  $\alpha$  values for specific models, budgets, or attention heads could yield finer optimization, it would also introduce significant search overhead and complicate deployment. Thus, we defer such granular adjustments to future work. Subsequent experiments and visual analyses further confirm that setting  $\alpha$  to 0.5 is a simple yet effective choice.

**Theorem 3.5.** Given the stage 1 selection  $\mathcal{N}'_i$ , the objective  $\mathcal{N}''_i$  of stage 2 is to minimize an upper bound  $\hat{\theta}$  of the output perturbation  $\mathcal{L}$ , using the remaining budget  $b'' = b - b'$ .

$$\begin{aligned} \arg \min_{\mathcal{N}''_i} \hat{\theta} \text{ where } \hat{\theta} &= C' - \left(2 - \frac{1}{\sigma}\right) \sum_{i=1}^n \mathcal{N}''_i A_i \|\mathbf{v}_{i,:}\|_1 \\ \text{subject to } \sum_{i=1}^n \mathcal{N}''_i &= b'', \\ C' &= C - \left(2 - \frac{1}{\sigma}\right) \sum_{i=1}^n \mathcal{N}'_i A_i \|\mathbf{v}_{i,:}\|_1. \end{aligned} \quad (13)$$

*Proof.* From Assumption 3.4, the first stage selection ensures:  $\sum_{i=1}^n \mathcal{N}_i A_i > \sum_{i=1}^n \mathcal{N}'_i A_i = \sigma > 0.5$ , leading to the inequality:  $2 - \frac{1}{\sum_{i=1}^n \mathcal{N}_i A_i} > 2 - \frac{1}{\sigma} > 0$ .

$$\begin{aligned} \theta &= C - \left(2 - \frac{1}{\sum_{i=1}^n \mathcal{N}_i A_i}\right) \sum_{i=1}^n (\mathcal{N}'_i + \mathcal{N}''_i) A_i \|\mathbf{v}_{i,:}\|_1 \\ &< C - \left(2 - \frac{1}{\sigma}\right) \sum_{i=1}^n \mathcal{N}'_i A_i \|\mathbf{v}_{i,:}\|_1 \\ &\quad - \left(2 - \frac{1}{\sigma}\right) \sum_{i=1}^n \mathcal{N}''_i A_i \|\mathbf{v}_{i,:}\|_1 \end{aligned} \quad (14)$$

Let  $C' = C - \left(2 - \frac{1}{\sigma}\right) \sum_{i=1}^n \mathcal{N}'_i A_i \|\mathbf{v}_{i,:}\|_1$ , then we can derive a new upper bound  $\hat{\theta}$  for  $\mathcal{L}$  factoring by second stage selection  $\mathcal{N}''_i$ :  $\theta < C' - \left(2 - \frac{1}{\sigma}\right) \sum_{i=1}^n \mathcal{N}''_i A_i \|\mathbf{v}_{i,:}\|_1 = \hat{\theta}$ . Thus, minimizing  $\hat{\theta}$  corresponds to selecting the  $b''$  entries with the highest values of  $\mathcal{A}_i = A_i \|\mathbf{v}_{i,:}\|_1$ , as implemented in the stage 2 selection (Algorithm 1).  $\square$

---

#### Algorithm 2 Observation Window Based Cache Eviction.

---

**Input:** All Query States  $Q \in \mathbb{R}^{n \times d_h}$ , KV Cache Entries  $K, V \in \mathbb{R}^{n \times d_h}$ , Window Size  $n'$

**Output:** Critical Cache Entries  $\hat{K}, \hat{V}$

```

1: allocating budget  $b$  for one head // AdaKV (Feng et al., 2024)
2:  $\hat{Q} = Q[-n' :, :]$ 
3:  $A = \text{softmax}(\hat{Q} K^T)$ 
4:  $\bar{A} = A.\text{mean}(\text{dim} = 0)$ 
5:  $\bar{A} = \text{maxpooling}(\bar{A})$  // SnapKV (Li et al., 2024)
6: if using regular selection then
7:   select  $b$  critical entries  $\hat{K}, \hat{V}$  by  $\text{Top}_k(\bar{A}', b)$ 
8: else if using our selection then
9:   select  $b$  critical entries  $\hat{K}, \hat{V}$  by Algorithm 1
10: end if
    return  $\hat{K}, \hat{V}$ 

```

---

Theorem 3.5 demonstrates that our second stage selection directly minimizes an upper bound of output perturbation for identifying critical cache entries. Unlike traditional strategies that rely solely on high attention weights for entry selection, the second stage of our algorithm jointly leverages both the attention weights and the value states projected through the parameter matrix, to directly constrain the worst-case output perturbation.

### 3.6. Integrating into SOTA cache eviction methods

We showcase the effectiveness of our algorithm by integrating it into existing cache eviction methods that rely on accumulated attention weights for selecting critical entries. Current SOTA cache eviction workflow is established by SnapKV (Li et al., 2024), which introduces an observation window mechanism to stably accumulate attention weights and employs the max pooling operations to avoid missing key information. Subsequent research (Zhang et al., 2024a; Feng et al., 2024) highlights the uneven distribution of critical cache entries across different heads, prompting the development of budget allocation strategies. The latest advancement, AdaKV (Feng et al., 2024), dynamically detects variations in critical KV cache entries across heads during runtime, allowing for flexible budget scheduling and improving output quality based on SnapKV. These two SOTA methods, SnapKV and AdaKV, can be unified as Algorithm 2, with two main components: budget allocation across heads (line 1) and the observation window and pooling mechanism for attention weight accumulation (lines 2–5). Our algorithm could integrate smoothly by replacing the original solely attention weight-based selection (lines 6–10).

## 4. Experiments

### 4.1. Models

We select two advanced open-source LLMs for evaluation: Mistral-7B-Instruct-v0.3 (Mistral-7B) (Jiang et al., 2023)

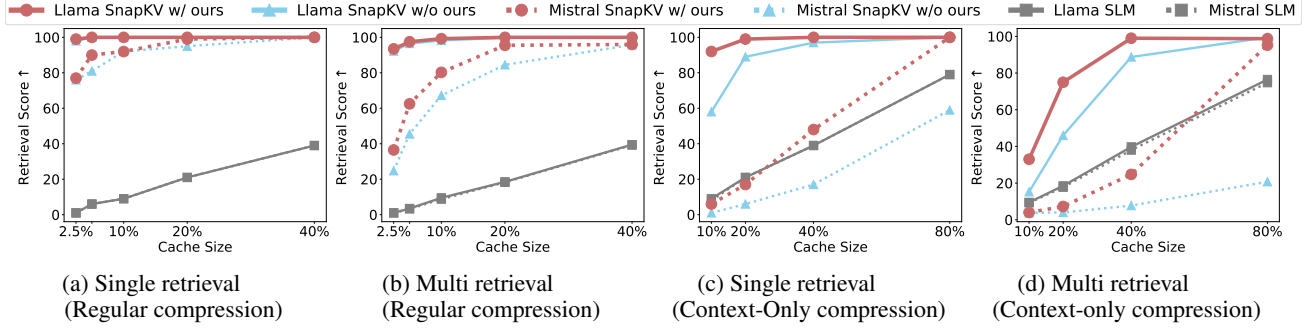


Figure 1: Needle-in-a-Haystack test(Integrated into SnapKV).

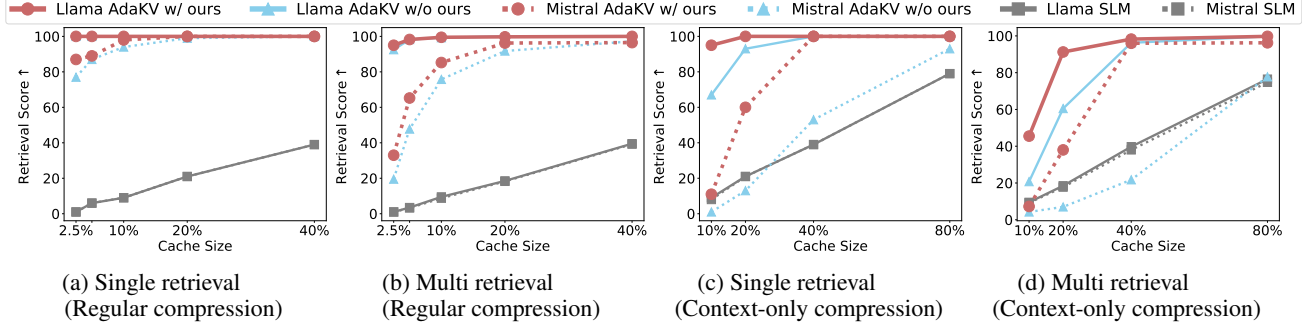


Figure 2: Needle-in-a-Haystack test(Integrated into AdaKV).

and Llama-3.1-8B-Instruct (Llama-3.1-8B) (Dubey et al., 2024), which support maximum sequence lengths of 32K and 128K, respectively.

## 4.2. Compression Scenario

We evaluate performance under two scenarios. The first is **regular compression** scenario, widely adopted in previous research (Li et al., 2024; Feng et al., 2024). In this scenario, question instructions are compressed alongside context, allowing for targeted compression for specific question. The second scenario is more challenging, referred to as **context-only compression** (NVIDIA, 2024). Here, only the context is provided during compression, with the problem instruction introduced afterward. This scenario is particularly relevant to more challenging tasks, such as multi-turn QA with long documents, where future questions cannot be anticipated during compression. For details, please refer to Appendix H.

## 4.3. Baselines

We integrated our algorithm with two cache eviction methods—SnapKV (Li et al., 2024) and AdaKV (Feng et al., 2024). These represent the current SOTA methods in Top-K-based and budget allocation-optimized eviction, respectively. By comparing the quality of their generated output before and after integration, we demonstrate the performance improvements our algorithm brings to these methods. The hyper-parameter  $\alpha$  in Algorithm 1 was set to 0.5 for all

experiments. Other fundamental settings for SnapKV and AdaKV were kept as originally defined, with a max-pooling kernel size of 7 and an observation window size of 32 (Feng et al., 2024). We also included earlier work based on the sliding window approach, such as StreamingLLM (SLM), which discards the KV Cache outside the current window. We use its performance as a reference.

## 4.4. Needle-in-a-Haystack Evaluation

In the Needle-in-a-Haystack test, a key sentence (the "needle") is inserted within a lengthy context (the "haystack") to evaluate the model's retrieval ability. Given the 32K context window limit of the Mistral model, we set the haystack length to 32K and create 100 test samples. The retrieval score is based on successful retrievals, with a maximum of 100. Following the Ruler settings (Hsieh et al., 2024), we conduct two tests: 1. Single-retrieval, where one sentence with a magic number is randomly inserted, requiring retrieval at the end. This simple task sees both full-cache Llama and Mistral scoring 100; 2. Multi-retrieval, where four sentences with magic numbers are inserted, requiring all to be retrieved. Here, full-cache Llama maintains a score of 100, while Mistral scores 97.

**Regular Compression.** Figures 1a, 1b, 2a and 2b show the results under regular compression. Whether using SnapKV or AdaKV, the Llama model exhibits strong retrieval capabilities, with only a slight drop in retrieval score in the multi-retrieval task when compressed to 2.5% cache size.

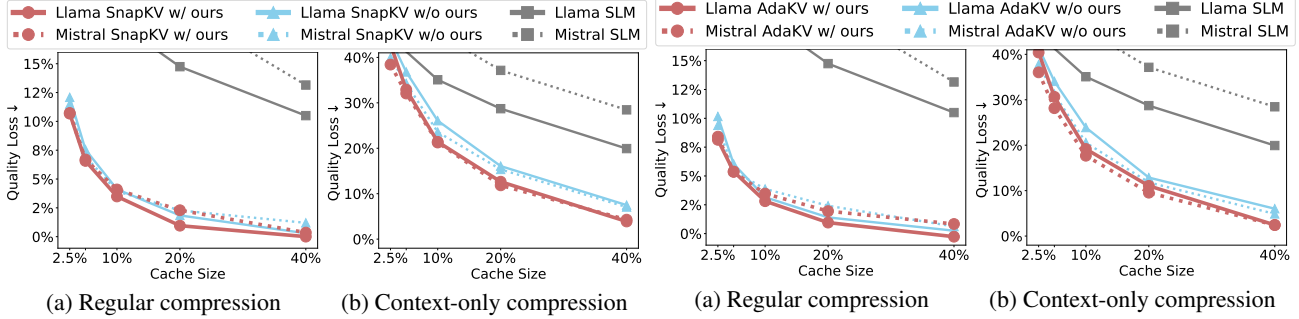


Table 1: Quality scores of Llama model on LongBench.

	Domain	6711 Full Cache	SnapKV $b = 20\%$		SnapKV $b = 40\%$		AdaKV $b = 20\%$		AdaKV $b = 40\%$	
			w/o ours	w/ ours	w/o ours	w/ ours	w/o ours	w/ ours	w/o ours	w/ ours
Llama-3.1-8B Regular	SingleDoc. QA	43.10	43.17	<b>43.23</b>	43.61	<b>43.63</b>	42.73	<b>43.05</b>	43.31	<b>43.59</b>
	MultiDoc. QA	46.49	46.63	<b>47.14</b>	<b>46.96</b>	46.64	<b>46.64</b>	46.42	<b>47.02</b>	46.97
	Summarization	28.97	25.35	<b>25.94</b>	27.05	<b>27.36</b>	25.49	<b>26.05</b>	27.24	<b>27.79</b>
	Fewshot	69.45	68.46	<b>68.59</b>	<b>69.43</b>	69.25	<b>69.19</b>	69.03	69.36	<b>69.40</b>
	Synthetic	53.73	53.07	<b>54.26</b>	53.77	<b>55.00</b>	53.56	<b>54.45</b>	53.96	<b>54.59</b>
	Code	57.86	57.88	<b>58.25</b>	58.12	<b>58.29</b>	58.43	<b>58.57</b>	58.27	<b>58.46</b>
	Ave.	49.20	48.29	<b>48.73</b>	49.06	<b>49.20</b>	48.51	<b>48.73</b>	49.08	<b>49.33</b>
Llama-3.1-8B Context-only	SingleDoc. QA	43.10	28.78	<b>30.43</b>	35.27	<b>38.27</b>	31.39	<b>32.74</b>	36.63	<b>39.24</b>
	MultiDoc. QA	46.49	33.51	<b>35.87</b>	40.50	<b>43.17</b>	34.90	<b>35.31</b>	41.36	<b>45.11</b>
	Summarization	28.97	23.82	<b>24.64</b>	26.11	<b>27.15</b>	24.29	<b>24.98</b>	26.66	<b>27.31</b>
	Fewshot	69.45	61.95	<b>63.04</b>	65.10	<b>66.87</b>	63.70	<b>64.74</b>	66.43	<b>68.19</b>
	Synthetic	53.73	48.19	<b>52.16</b>	53.17	<b>54.22</b>	50.39	<b>52.30</b>	53.00	<b>53.60</b>
	Code	57.86	60.05	<b>60.75</b>	60.49	<b>60.91</b>	61.14	<b>61.16</b>	60.30	<b>60.60</b>
	Ave.	49.20	41.29	<b>42.99</b>	45.52	<b>47.29</b>	42.87	<b>43.77</b>	46.24	<b>48.00</b>

Our algorithm improves performance where existing methods show losses and maintains lossless scores in other cases. However, for models like Mistral, which face challenges in handling long-context processing, KV cache compression significantly affects retrieval performance, particularly in the multi-retrieval task. In such cases, integrating our algorithm with existing methods significantly enhances performance. For instance, as shown in Figure 1b, our approach raises the retrieval score from 84.5 to 95.5 when paired with SnapKV at 20% cache size in the Mistral model. Similarly, in Figure 2b, integrating with the more advanced AdaKV method achieves a comparable improvement, increasing scores from 91.75 to 96.25.

**Context-only Compression.** In the context-only compression scenario, the model is unaware of future questions during compression, making it difficult to assess the importance for specific queries. As a result, both eviction methods on Llama and Mistral models show a significant drop in retrieval scores, as illustrated in Figures 1c, 1d, 2c, and 2d. In this case, the advantages of our method become particularly evident. Using the advanced AdaKV method as a reference, our algorithm achieves substantial improvements. For the Llama model with a 20% cache size, it raises the single

retrieval score from 93 to 100 (Figure 2c) and the multi retrieval score from 60.5 to 91.25 (Figure 2d). Similarly, for the Mistral model with a 40% cache size, our approach boosts the single retrieval score from 53 to 100 (Figure 2c) and the multi-retrieval score from 21.75 to 96 (Figure 2d), achieving up to a 4.41x improvement.

#### 4.5. LongBench Evaluation

For a comprehensive evaluation, we incorporated the real-world task benchmark LongBench, consisting of 16 datasets across six task domains: single-document QA, multi-document QA, summarization, few-shot learning, synthetic, and code generation. For each dataset, we apply the LongBench-recommended metrics for quality assessment. Detailed information for each dataset can be found in Appendix D.

**Overview.** Figures 3 and 4 illustrate the average quality loss of different methods across 16 datasets in Longbench. As the cache size increases, the quality loss for all compression methods gradually decreases to near-lossless. Notably, the Top-K eviction methods, SnapKV and AdaKV, consistently outperform the sliding window method, StreamingLLM, in both the regular and context-only compression scenarios.

However, these two different compression scenarios exhibit significantly different compression losses. For instance, in Figure 4a, AdaKV shows only around 1.4% and 2.4% quality loss with a 20% cache size in Llama and Mistral, whereas in Figure 4b, the more challenging context-only compression scenario results in higher quality losses of 12.9% and 11.8%, respectively. Our method effectively reduces the losses of existing methods in both scenarios. For example, with a 20% cache size in the Llama model, when integrated with SnapKV, our method reduces the losses in both the regular and context-only scenarios from 1.8% and 16% to 0.9% and 13%. When combined with AdaKV, it reduces the original losses of 1.4% and to 13% to 1% and 11%, respectively.

**Task domain analysis** Tables 1 present a detailed overview of the Llama model’s scores across various task domains in both regular and context-only compression scenarios when our algorithm is integrated into SnapKV and AdaKV on two cache sizes (20% and 40%). Due to space constraints, the corresponding scores for the Mistral model are available in Appendix C. In the regular compression scenario, where original cache eviction results in minimal loss, all methods achieve scores close to the full cache case. Even in this situation, our algorithm enhances quality in 19 out of 24 task domains with two cache size of two base methods, demonstrating its effectiveness. In the more challenging context-only compression scenario, the quality loss from original SnapKV and AdaKV compression provides ample room for optimization by our algorithm, ultimately achieving higher scores across all 24 task domains. This indicates that our method is task-agnostic for enhancing the quality of existing cache eviction methods.

#### 4.6. Analysis of Practical Output Perturbation

We empirically evaluate our algorithm’s effectiveness in reducing practical output perturbation using the Multi-News dataset, which comprises 200 summarization samples. Tracking the hidden states of the first, third, and fifth decoding tokens with a 20% cache size, we visualize output perturbations with and without our algorithm using the SnapKV method (additional results in Appendix B).

**Head-wise Analysis:** Our algorithm significantly reduces head-wise average output perturbation across all samples in the Llama model, achieving lower perturbations in 92%, 92%, and 95% of attention heads for tokens 1, 2, and 3, respectively (Figure 5).

**Layer-wise Analysis:** Figure 6 shows how our algorithm progressively reduces perturbation across layers, leading to substantial decreases in the final layer, which directly impacts the generated token vocabulary distribution.

**Budget-wise Analysis:** Figure 7 illustrates that our method

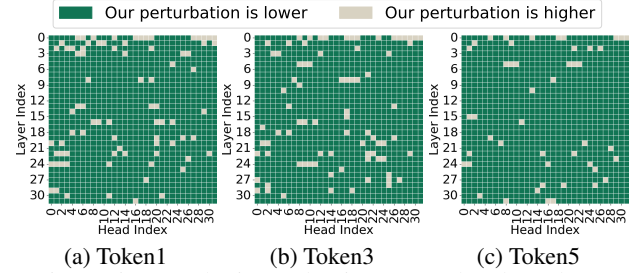


Figure 5: Perturbation reduction across heads. (Llama)

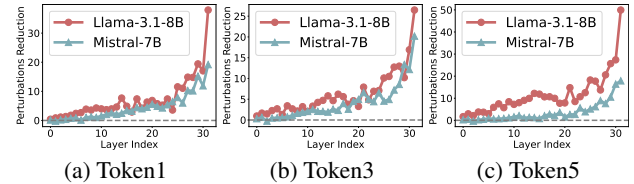


Figure 6: Perturbation reduction across layers.

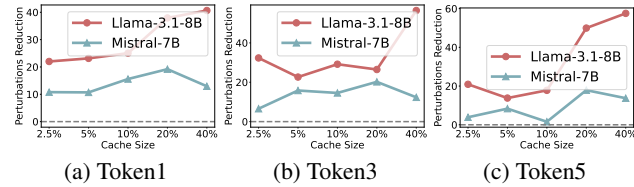


Figure 7: Perturbation reduction across budgets.

effectively lowers output perturbation across different cache sizes from 2.5% to 40%, underscoring its robustness of varying budget constraints in real world application.

These analyses demonstrate that our method robustly reduces practical output perturbation by theoretically constraining worst-case perturbation by Algorithm 1. This results in the post-eviction output hidden states that are more consistent with those from the full KV cache, thereby enhancing generation consistency and reducing quality loss.

## 5. Conclusion

In this paper, we pinpoint a key limitation in current cache eviction methods: the reliance on intuitive heuristics of using attention weights to select critical cache entries for eviction. For the first time, we formalize the problem of critical cache entry selection from the perspective of output perturbation and provide a theoretical analysis. Furthermore, we propose a novel algorithm based on constraining output perturbation in the worst-case for critical cache selection, which is then integrated into existing SOTA cache eviction methods. Comprehensive evaluations using 2 cases of Needle-in-a-Haystack test and 16 datasets from Longbench demonstrate that our algorithm improves the performance of advanced cache eviction methods, across different budget constraints. Further empirical analysis also confirms and explains this benefit from the perspective of practical output perturbation: our algorithm consistently yields lower perturbation compared to previous methods that rely solely on attention weights, in various settings.

## Impact Statement

This paper presents work whose goal is to advance the field of Machine Learning. There are many potential societal consequences of our work, none which we feel must be specifically highlighted here.

## References

- Achiam, J., Adler, S., Agarwal, S., Ahmad, L., Akkaya, I., Aleman, F. L., Almeida, D., Altenschmidt, J., Altman, S., Anadkat, S., et al. Gpt-4 technical report. *arXiv preprint arXiv:2303.08774*, 2023.
- Adnan, M., Arunkumar, A., Jain, G., Nair, P., Soloveychik, I., and Kamath, P. Keyformer: Kv cache reduction through key tokens selection for efficient generative inference. *Proceedings of Machine Learning and Systems*, 6:114–127, 2024.
- Bai, Y., Lv, X., Zhang, J., Lyu, H., Tang, J., Huang, Z., Du, Z., Liu, X., Zeng, A., Hou, L., et al. Longbench: A bilingual, multitask benchmark for long context understanding. *arXiv preprint arXiv:2308.14508*, 2023.
- Bai, Y., Lv, X., Zhang, J., Lyu, H., Tang, J., Huang, Z., Du, Z., Liu, X., Zeng, A., Hou, L., Dong, Y., Tang, J., and Li, J. Longbench: A bilingual, multitask benchmark for long context understanding, 2024. URL <https://arxiv.org/abs/2308.14508>.
- Dasigi, P., Lo, K., Beltagy, I., Cohan, A., Smith, N. A., and Gardner, M. A dataset of information-seeking questions and answers anchored in research papers. *arXiv preprint arXiv:2105.03011*, 2021.
- Davis, J. Q., Gu, A., Choromanski, K., Dao, T., Re, C., Finn, C., and Liang, P. Catformer: Designing stable transformers via sensitivity analysis. In Meila, M. and Zhang, T. (eds.), *Proceedings of the 38th International Conference on Machine Learning*, volume 139 of *Proceedings of Machine Learning Research*, pp. 2489–2499. PMLR, 18–24 Jul 2021. URL <https://proceedings.mlr.press/v139/davis21a.html>.
- Dubey, A., Jauhri, A., Pandey, A., Kadian, A., Al-Dahle, A., Letman, A., Mathur, A., Schelten, A., Yang, A., Fan, A., et al. The llama 3 herd of models. *arXiv preprint arXiv:2407.21783*, 2024.
- Fabbri, A. R., Li, I., She, T., Li, S., and Radev, D. R. Multi-news: A large-scale multi-document summarization dataset and abstractive hierarchical model. *arXiv preprint arXiv:1906.01749*, 2019.
- Feng, Y., Lv, J., Cao, Y., Xie, X., and Zhou, S. K. Adakv: Optimizing kv cache eviction by adaptive budget allocation for efficient llm inference, 2024. URL <https://arxiv.org/abs/2407.11550>.
- Frantar, E. and Alistarh, D. Sparsegpt: Massive language models can be accurately pruned in one-shot. In *International Conference on Machine Learning*, pp. 10323–10337. PMLR, 2023.
- Ge, S., Zhang, Y., Liu, L., Zhang, M., Han, J., and Gao, J. Model tells you what to discard: Adaptive KV cache compression for LLMs. In *The Twelfth International Conference on Learning Representations*, 2024a. URL <https://openreview.net/forum?id=uNrFpDPMYo>.
- Ge, S., Zhang, Y., Liu, L., Zhang, M., Han, J., and Gao, J. Model tells you what to discard: Adaptive kv cache compression for llms, 2024b. URL <https://arxiv.org/abs/2310.01801>.
- Gliwa, B., Mochol, I., Biesek, M., and Wawer, A. Samsun corpus: A human-annotated dialogue dataset for abstractive summarization. *arXiv preprint arXiv:1911.12237*, 2019.
- Gu, Q. Llm-based code generation method for golang compiler testing. In *Proceedings of the 31st ACM Joint European Software Engineering Conference and Symposium on the Foundations of Software Engineering*, pp. 2201–2203, 2023.
- Guo, D., Xu, C., Duan, N., Yin, J., and McAuley, J. Longcoder: A long-range pre-trained language model for code completion, 2023. URL <https://arxiv.org/abs/2306.14893>.
- Han, S., Pool, J., Tran, J., and Dally, W. Learning both weights and connections for efficient neural network. *Advances in neural information processing systems*, 28, 2015.
- Ho, X., Duong Nguyen, A.-K., Sugawara, S., and Aizawa, A. Constructing a multi-hop QA dataset for comprehensive evaluation of reasoning steps. In Scott, D., Bel, N., and Zong, C. (eds.), *Proceedings of the 28th International Conference on Computational Linguistics*, pp. 6609–6625, Barcelona, Spain (Online), December 2020. International Committee on Computational Linguistics. doi: 10.18653/v1/2020.coling-main.580. URL <https://aclanthology.org/2020.coling-main.580>.
- Hooper, C., Kim, S., Mohammadzadeh, H., Mahoney, M. W., Shao, Y. S., Keutzer, K., and Gholami, A. Kvquant: Towards 10 million context length llm inference with kv cache quantization. *arXiv preprint arXiv:2401.18079*, 2024.

- Hsieh, C.-P., Sun, S., Krizan, S., Acharya, S., Rekesh, D., Jia, F., Zhang, Y., and Ginsburg, B. Ruler: What’s the real context size of your long-context language models? *arXiv preprint arXiv:2404.06654*, 2024.
- Huang, L., Cao, S., Parulian, N., Ji, H., and Wang, L. Efficient attentions for long document summarization. *arXiv preprint arXiv:2104.02112*, 2021.
- Jiang, A. Q., Sablayrolles, A., Mensch, A., Bamford, C., Chaplot, D. S., Casas, D. d. l., Bressand, F., Lengyel, G., Lample, G., Saulnier, L., et al. Mistral 7b. *arXiv preprint arXiv:2310.06825*, 2023.
- Jiang, H., Li, Y., Zhang, C., Wu, Q., Luo, X., Ahn, S., Han, Z., Abdi, A. H., Li, D., Lin, C.-Y., Yang, Y., and Qiu, L. Minference 1.0: Accelerating pre-filling for long-context llms via dynamic sparse attention, 2024. URL <https://arxiv.org/abs/2407.02490>.
- Joshi, M., Choi, E., Weld, D. S., and Zettlemoyer, L. Triviaqa: A large scale distantly supervised challenge dataset for reading comprehension, 2017. URL <https://arxiv.org/abs/1705.03551>.
- Kamradt, G. Needle In A Haystack - pressure testing LLMs. *Github*, 2023. URL [https://github.com/gkamradt/LLMTest\\_NeedleInAHaystack/tree/main](https://github.com/gkamradt/LLMTest_NeedleInAHaystack/tree/main).
- Kočíšký, T., Schwarz, J., Blunsom, P., Dyer, C., Hermann, K. M., Melis, G., and Grefenstette, E. The narrativeqa reading comprehension challenge. *Transactions of the Association for Computational Linguistics*, 6:317–328, 2018.
- Li, X. and Roth, D. Learning question classifiers. In *COLING 2002: The 19th International Conference on Computational Linguistics*, 2002.
- Li, Y., Huang, Y., Yang, B., Venkitesh, B., Locatelli, A., Ye, H., Cai, T., Lewis, P., and Chen, D. Snapkv: Llm knows what you are looking for before generation. *arXiv preprint arXiv:2404.14469*, 2024.
- Liu, L., Liu, X., Gao, J., Chen, W., and Han, J. Understanding the difficulty of training transformers. In Webber, B., Cohn, T., He, Y., and Liu, Y. (eds.), *Proceedings of the 2020 Conference on Empirical Methods in Natural Language Processing (EMNLP)*, pp. 5747–5763, Online, November 2020. Association for Computational Linguistics. doi: 10.18653/v1/2020.emnlp-main.463. URL <https://aclanthology.org/2020.emnlp-main.463>.
- Liu, T., Xu, C., and McAuley, J. Repobench: Benchmarking repository-level code auto-completion systems, 2023. URL <https://arxiv.org/abs/2306.03091>.
- Liu, Z., Desai, A., Liao, F., Wang, W., Xie, V., Xu, Z., Kyrillidis, A., and Shrivastava, A. Scissorhands: Exploiting the persistence of importance hypothesis for llm kv cache compression at test time. *Advances in Neural Information Processing Systems*, 36, 2024a.
- Liu, Z., Yuan, J., Jin, H., Zhong, S., Xu, Z., Braverman, V., Chen, B., and Hu, X. Kivi: A tuning-free asymmetric 2bit quantization for kv cache. *arXiv preprint arXiv:2402.02750*, 2024b.
- Lv, J., Feng, Y., Xie, X., Jia, X., Peng, Q., and Xie, G. Critiprefill: A segment-wise criticality-based approach for prefilling acceleration in llms, 2024. URL <https://arxiv.org/abs/2409.12490>.
- NVIDIA. Kvpres, 2024. URL <https://github.com/NVIDIA/kvpres>.
- Sun, H., Chen, Z., Yang, X., Tian, Y., and Chen, B. Tri-force: Lossless acceleration of long sequence generation with hierarchical speculative decoding. *arXiv preprint arXiv:2404.11912*, 2024a.
- Sun, M., Liu, Z., Bair, A., and Kolter, J. Z. A simple and effective pruning approach for large language models. In *The Twelfth International Conference on Learning Representations*, 2024b. URL <https://openreview.net/forum?id=PxoFut3dWW>.
- Tang, J., Zhao, Y., Zhu, K., Xiao, G., Kasikci, B., and Han, S. Quest: Query-aware sparsity for efficient long-context llm inference. *arXiv preprint arXiv:2406.10774*, 2024a.
- Tang, J., Zhao, Y., Zhu, K., Xiao, G., Kasikci, B., and Han, S. Quest: Query-aware sparsity for efficient long-context llm inference, 2024b. URL <https://arxiv.org/abs/2406.10774>.
- Trivedi, H., Balasubramanian, N., Khot, T., and Sabharwal, A. Musique: Multihop questions via single-hop question composition. *Transactions of the Association for Computational Linguistics*, 10:539–554, 2022.
- Wang, L., Ma, C., Feng, X., Zhang, Z., Yang, H., Zhang, J., Chen, Z., Tang, J., Chen, X., Lin, Y., Zhao, W. X., Wei, Z., and Wen, J. A survey on large language model based autonomous agents. *Frontiers of Computer Science*, 18(6), March 2024. ISSN 2095-2236. doi: 10.1007/s11704-024-40231-1. URL <http://dx.doi.org/10.1007/s11704-024-40231-1>.
- Xiao, G., Tian, Y., Chen, B., Han, S., and Lewis, M. Efficient streaming language models with attention sinks. *arXiv preprint arXiv:2309.17453*, 2023.

- Yang, D., Han, X., Gao, Y., Hu, Y., Zhang, S., and Zhao, H. Pyramidinfer: Pyramid kv cache compression for high-throughput llm inference. *Association for Computational Linguistics*, 2024.
- Yang, Z., Qi, P., Zhang, S., Bengio, Y., Cohen, W. W., Salakhutdinov, R., and Manning, C. D. Hotpotqa: A dataset for diverse, explainable multi-hop question answering. *arXiv preprint arXiv:1809.09600*, 2018.
- Yi, Z., Ouyang, J., Liu, Y., Liao, T., Xu, Z., and Shen, Y. A survey on recent advances in llm-based multi-turn dialogue systems. *arXiv preprint arXiv:2402.18013*, 2024.
- Zhang, Y., Gao, B., Liu, T., Lu, K., Xiong, W., Dong, Y., Chang, B., Hu, J., Xiao, W., et al. Pyramidkv: Dynamic kv cache compression based on pyramidal information funneling. *arXiv preprint arXiv:2406.02069*, 2024a.
- Zhang, Z., Sheng, Y., Zhou, T., Chen, T., Zheng, L., Cai, R., Song, Z., Tian, Y., Ré, C., Barrett, C., et al. H2o: Heavy-hitter oracle for efficient generative inference of large language models. *Advances in Neural Information Processing Systems*, 36, 2024b.
- Zhong, M., Yin, D., Yu, T., Zaidi, A., Mutuma, M., Jha, R., Awadallah, A. H., Celikyilmaz, A., Liu, Y., Qiu, X., et al. Qmsum: A new benchmark for query-based multi-domain meeting summarization. *arXiv preprint arXiv:2104.05938*, 2021.

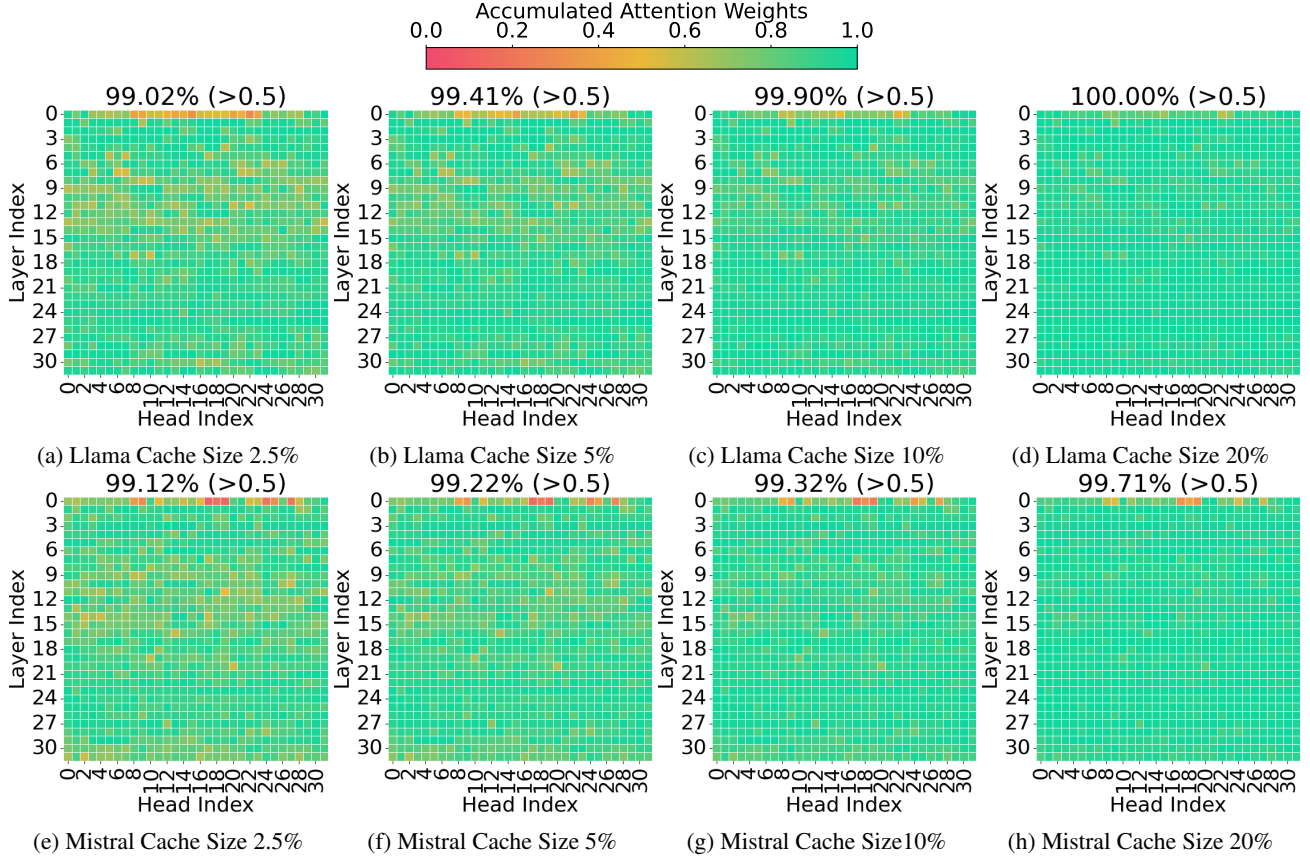


Figure 8: Accumulated attention weights: Assumption 3.4 validates in over 99% of heads across various cache sizes.

## A. Validation of Assumption 3.4

We ensure the reliability of Assumption 3.4 by analyzing the cumulative attention weights of critical KV Cache entries  $\sum_{i=1}^n \mathcal{N}_i A_i$  in individual heads. As shown in Figure 8, for varying models and budget levels, the majority of attention heads can effectively accumulate over half of the attention weights. The only exceptions are a few attention heads in the first layer. This is primarily due to the low sparsity of attention weights in certain heads of the first layer, a phenomenon that has been noted in many related studies (Tang et al., 2024a; Zhang et al., 2024b;a). This observation aligns with the fact that certain heads in the first layer violate Assumption 3.4, which may lead our algorithm to increase the output perturbation of these heads as shown in Figure 5. However, this is not a significant issue in our current algorithm, as these heads constitute less than 1% of the total, and their negative impact is easily offset by the gains from other heads, resulting in substantial overall benefits. A potential solution to this issue is to set the algorithm’s threshold  $\alpha$  based on the characteristics of each head to achieve greater benefits. However, considering the additional complexity this approach might introduce, especially given the potential impact of different cache sizes and models, we leave this further optimization for future research.

## B. Additional Empirical Analysis

Figure 9 provides a visualization of the reduced perturbations achieved by our algorithm across different heads in the Mistral model, demonstrating its continued effectiveness. We then present a more detailed visual analysis to support the conclusions in the main paper. Figures 10 11 illustrate the reduced perturbation when combining AdaKV with our algorithm under various layers and budgets. Clearly, in all scenarios, our algorithm significantly reduces output perturbation of AdaKV after cache eviction, resulting in lower quality loss and improved final generation quality.

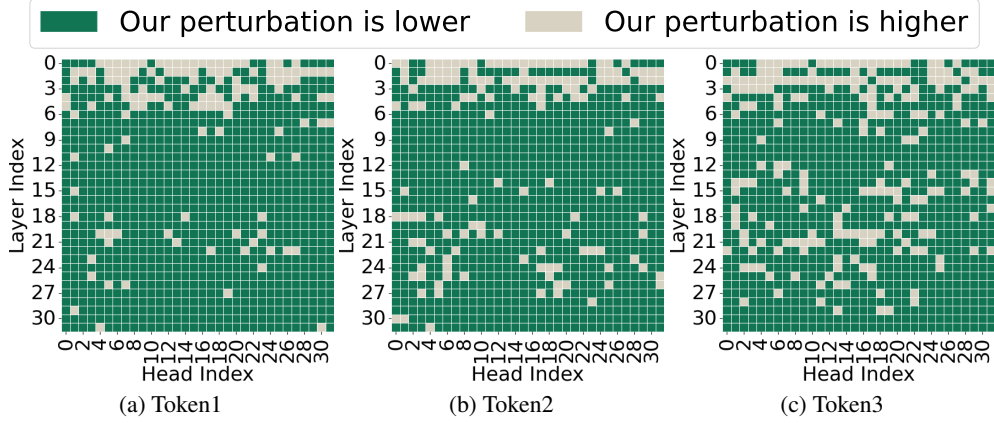


Figure 9: Perturbation reduction across heads. (Mistral)

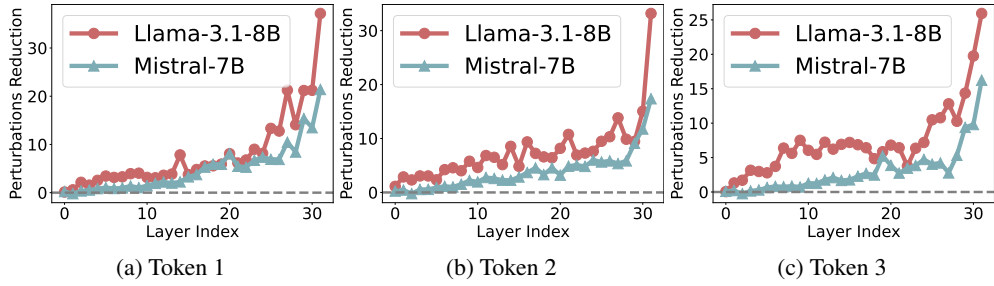


Figure 10: Perturbation reduction across layers on AdaKV.

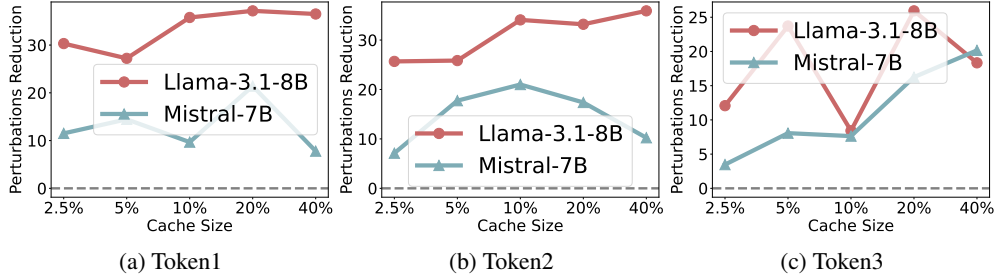


Figure 11: Perturbation reduction across budgets on AdaKV.

### C. Task Domain Analysis of Longbench Results on Mistral Model

Table 2 presents the performance of the Mistral model on the LongBench benchmark. It shows that our enhanced cache eviction method improves the quality across various task domains. In the context-only compression scenario, the enhanced method shows improvements in 22 out of 24 task domains, while in the regular compression scenario, 18 domains show improvements, demonstrating a clear advantage.

### D. Details of 16 Datasets in Longbench

As a widely used long-context benchmark (Feng et al., 2024; Li et al., 2024; Zhang et al., 2024a), LongBench consists of 16 datasets across six task domains: single-document question answering (QA) (Kočísky et al., 2018; Dasigi et al., 2021), multi-document QA (Yang et al., 2018; Ho et al., 2020; Trivedi et al., 2022), summarization (Huang et al., 2021; Zhong et al., 2021; Fabbri et al., 2019), few-shot learning (Joshi et al., 2017; Gliwa et al., 2019; Li & Roth, 2002), synthetic tasks (Bai et al., 2023), and code generation (Guo et al., 2023; Liu et al., 2023). The average token length across all 16 datasets is 6,711. Table 3 provides detailed information on the 16 datasets in LongBench.

Table 2: LongBench results on Mistral model.

	Domain	6711 Full Cache	SnapKV $b = 20\%$		SnapKV $b = 40\%$		AdaKV $b = 20\%$		AdaKV $b = 40\%$	
			w/o ours	w/ ours	w/o ours	w/ ours	w/o ours	w/ ours	w/o ours	w/ ours
Mistral-7B Regular	Single-Doc. QA	38.37	25.13	<b>28.24</b>	31.64	<b>34.33</b>	27.25	<b>29.06</b>	33.42	<b>36.06</b>
	Multi-Doc. QA	39.40	29.64	<b>32.07</b>	33.57	<b>36.61</b>	31.71	<b>33.04</b>	35.97	<b>38.00</b>
	Summarization	28.76	24.18	<b>24.61</b>	26.24	<b>26.94</b>	24.18	<b>24.83</b>	26.24	<b>27.06</b>
	Few-shot	70.33	63.89	<b>65.54</b>	67.95	<b>68.57</b>	66.00	<b>67.08</b>	68.67	<b>69.79</b>
	Synthetic	52.50	45.25	<b>46.53</b>	49.75	<b>51.05</b>	48.00	<b>49.25</b>	50.75	<b>50.84</b>
	Code	61.25	61.40	<b>61.94</b>	62.06	62.06	62.55	<b>62.56</b>	<b>63.35</b>	62.68
	Ave.	47.38	40.11	<b>41.77</b>	44.03	<b>45.35</b>	41.78	<b>42.85</b>	45.07	<b>46.23</b>
Mistral-7B Context-only	Single-Doc. QA	38.37	<b>37.85</b>	37.42	37.97	<b>38.12</b>	36.98	<b>37.27</b>	<b>38.40</b>	37.71
	Multi-Doc. QA	39.40	37.67	<b>38.06</b>	38.75	<b>39.37</b>	38.00	<b>38.08</b>	<b>39.39</b>	39.23
	Summarization	28.76	25.99	<b>26.28</b>	27.19	<b>27.80</b>	26.00	<b>26.29</b>	27.48	<b>27.82</b>
	Few-shot	70.33	70.15	<b>70.23</b>	70.23	<b>70.68</b>	70.12	<b>70.44</b>	70.46	<b>70.72</b>
	Synthetic	52.50	<b>51.75</b>	51.03	51.75	<b>52.05</b>	51.75	<b>52.00</b>	<b>51.75</b>	51.34
	Code	61.25	61.15	<b>61.30</b>	61.52	<b>61.67</b>	61.47	<b>61.52</b>	<b>61.34</b>	61.30
	Ave.	47.38	<b>46.30</b>	46.29	46.81	<b>47.21</b>	46.23	<b>46.45</b>	<b>47.08</b>	46.98

Table 3: Details of 16 datasets in LongBench.

Task	Task Type	Eval metric	Avg len	Language	Sample Num
NarrativeQA	Single-Doc. QA	F1	18,409	EN	200
Qasper	Single-Doc. QA	F1	3,619	EN	200
MultiFieldQA-en	Single-Doc. QA	F1	4,559	EN	150
HotpotQA	Multi-Doc. QA	F1	9,151	EN	200
2WikiMultiHopQA	Multi-Doc. QA	F1	4,887	EN	200
MuSiQue	Multi-Doc. QA	F1	11,214	EN	200
GovReport	Summarization	Rouge-L	8,734	EN	200
QMSum	Summarization	Rouge-L	10,614	EN	200
MultiNews	Summarization	Rouge-L	2,113	EN	200
TREC	Few-shot Learning	Accuracy	5,177	EN	200
TriviaQA	Few-shot Learning	F1	8,209	EN	200
SAMSum	Few-shot Learning	Rouge-L	6,258	EN	200
PassageCount	Synthetic	Accuracy	11,141	EN	200
PassageRetrieval-en	Synthetic	Accuracy	9,289	EN	200
LCC	Code	Edit Sim	1,235	Python/C#/Java	500
RepoBench-P	Code	Edit Sim	4,206	Python/Java	500

## E. Analysis of Previous Solely Attention Weights-Based Selection from a Perturbation Perspective

Our algorithm differs from the previous solely attention weights-based selection method primarily in Stage 2. Specifically, by modifying stage 2 of our algorithm to perform the same attention weights-based selection operation as in stage 1, our approach will degrade into the previous method. This modification allows us to conveniently apply perturbation-constrained theory to analyze the earlier attention weights-based selection strategy.

**Theorem E.1.** *Previous solely attention weights-based selection is equivalent to minimizing another upper bound  $\hat{\theta}^{relax}$ , a relaxed form of  $\hat{\theta}$ , with remaining budget  $b'$  based on stage 1 selection.*

$$\hat{\theta}^{relax} = C' - M \left( 2 - \frac{1}{\sigma} \right) \sum_{i=1}^n \mathcal{N}_i'' A_i \quad \text{where} \quad M = MIN(\|\mathbf{v}_{i,:}\|_1) \quad (15)$$

*Proof.* We relax the upper bound  $\hat{\theta}$  by utilizing  $M = MIN(\|\mathbf{v}_{i,:}\|_1)$ :

$$\hat{\theta} = C' - \left( 2 - \frac{1}{\sigma} \right) \sum_{i=1}^n \mathcal{N}_i'' A_i \|\mathbf{v}_{i,:}\|_1 \leq C' - M \left( 2 - \frac{1}{\sigma} \right) \sum_{i=1}^n \mathcal{N}_i'' A_i = \hat{\theta}^{relax} \quad (16)$$

In the solely attention weights-based selection strategy, the  $\mathcal{N}''$  selection is performed using  $Top - K(A_i, b'')$  to maximize  $\sum_{i=1}^n \mathcal{N}_i'' A_i$ . This is therefore equivalent to minimizing the relaxed upper bound,  $\hat{\theta}^{relax}$ .

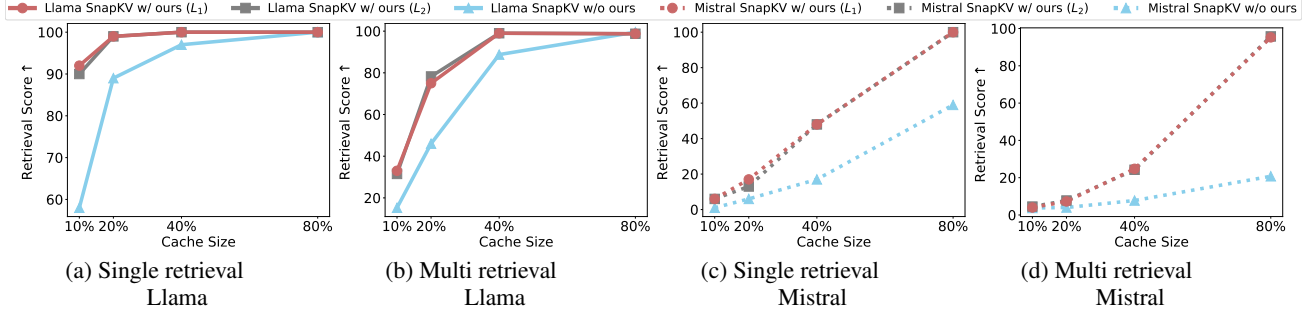


Figure 12: Choice of Distance Metric:  $L_1$  distance and  $L_2$  distance. (SnapKV)

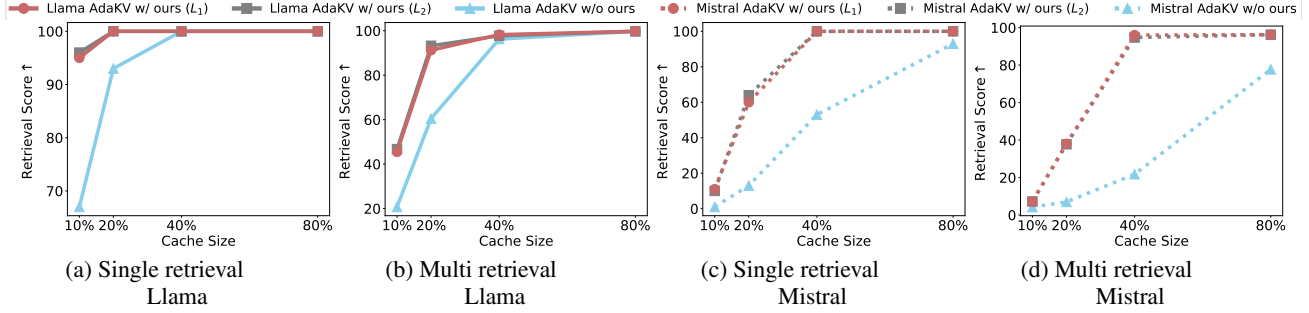


Figure 13: Choice of Distance Metric:  $L_1$  distance and  $L_2$  distance. (AdaKV)

□

Theorem E.1 demonstrates that the solely attention weights-based selection strategy is equivalent to minimizing the relaxed upper bound  $\hat{\theta}^{relax}$ . In contrast, our algorithm optimizes a tighter upper bound,  $\theta$ . While this does not guarantee that our approach will yield a strictly better solution, intuitively, an algorithm designed to optimize a tighter bound often achieves better results. Theorem E.1 also provides some insight into why a critical KV Cache subset can replace the entire KV Cache in cache eviction methods. Due to the power-law distribution of attention weights (Zhang et al., 2024b), removing most cache entries with near-zero attention weights has a negligible impact on this upper bound. Consequently, the perturbation to the actual output is also bounded by this upper bound.

## F. Choice of Distance Metric

As demonstrated in preliminary evaluations shown in Figures 12 and 13, both  $L_1$  and  $L_2$  distance-based perturbation-constrained selection algorithms effectively enhance the retrieval scores of original SnapKV and AdaKV. However, we don't observe notable quality improvements when using the  $L_2$  distance compared to the simpler  $L_1$  distance. Additionally, the  $L_1$  distance provides advantages in terms of simplicity and greater stability in half-precision floating-point computations. Thus, we adopt the  $L_1$  distance metric in this paper for our analysis. Future work could explore more complex distance metrics within our framework, offering a promising research direction.

## G. Additional Related Works

Sparse attention methods (Jiang et al., 2024; Tang et al., 2024b; Lv et al., 2024) are conceptually related to the KV cache eviction methods discussed in this paper. While KV cache eviction retains only a small subset of essential KV cache entries, sparse attention methods maintain all entries during inference. However, during computation, only the most critical entries are selectively utilized in the sparse attention mechanism. Consequently, sparse attention methods do not reduce the memory footprint of the KV cache but enhance inference speed and often offer better output quality than cache eviction methods (Tang et al., 2024b). Existing sparse attention methods typically rely on approximate estimations of attention weights to identify critical entries (Tang et al., 2024b; Lv et al., 2024). Future works could explore integrating our proposed perturbation-constrained selection algorithm to refine these methods by achieving more accurate critical cache entry identification.

Some adaptive methods in KV cache eviction or sparse attention, such as (Ge et al., 2024b; Jiang et al., 2024), employ varying critical cache selection strategies tailored to the characteristics of different attention heads. For example, some heads use attention weights based selection, while others utilize fixed patterns, such as recent window-based or special token-based approaches. Our method can also be applied to enhance performance in the head which according to attention weights-based selection strategies, providing a boost to adaptive methods.

KV cache quantization refers to the application of quantization techniques to reduce the size of the KV cache by lowering the precision of individual cache entries (Liu et al., 2024b; Hooper et al., 2024). For example, this can involve quantizing the original 16-bit KV cache entries to 4-bit or 2-bit precision. However, these methods typically retain all cache entries, making them fundamentally orthogonal to the cache eviction methods explored in this paper.

## H. Prompt Templates for Ruler and LongBench in Regular and Context-only Compression Scenarios

Below are prompt templates for various tasks. We assess performance under two scenarios: regular compression and context-only compression. We adhere to the input prompt format from KVPress (NVIDIA, 2024), dividing the input into context and question segments. The question segment is highlighted in green, while other colors represent the context segment. In regular compression, both the context and question segments are input into the model and compressed. For context-only compression, where future questions are unpredictable, only the context segment is input for compression. After compression, the question segment is input for answer generation.

### H.1. NIAH Template

In the Needle-in-A-Haystack task, a keyword, referred to as the "needle", is embedded within a lengthy context known as the "haystack". The objective of this task is to extract the "needle" from the "haystack", which is composed of essays by Paul Graham (Kamradt, 2023).

For the Single Needle-in-A-Haystack(S-NIAH) task, the goal is to retrieve a single "needle". Similarly, the Multi-Value Needle-in-A-Haystack(MV-NIAH) task requires the extraction of multiple inserted "needles". To prevent models from refusing to answer our questions, we append the answer prefix to the input, prompting the models to generate answers.

Table 4: Single retrieval and multi retrieval templates in Needle-in-A-Haystack tests.

Single retrieval	<p><b>Task Template:</b> Some special magic numbers are hidden within the following text. Make sure to memorize it. I will quiz you about the numbers afterwards. Paul Graham Essays. ..... One of the special magic numbers for {word} is: {number}. .... What is the special magic number for {word} mentioned in the provided text?</p> <p>The special magic number for {word} mentioned in the provided text is</p>
Multi retrieval	<p><b>Task Template:</b> Some special magic numbers are hidden within the following text. Make sure to memorize it. I will quiz you about the numbers afterwards. Paul Graham Essays. ..... One of the special magic numbers for {word} is: {number-1}. .... ..... One of the special magic numbers for {word} is: {number-2}. .... ..... One of the special magic numbers for {word} is: {number-3}. .... ..... One of the special magic numbers for {word} is: {number-4}. .... What are all the special magic numbers for {word} mentioned in the provided text?</p> <p>The special magic numbers for {word} mentioned in the provided text are</p>

### H.2. LongBench Template

The construction of the LongBench template follows the official formats (Bai et al., 2024) to evaluate performance under regular compression and context-only compression.

Table 5: LongBench templates. Single-Doc. QA Tasks.

NarrativeQA	<p><b>Task Template:</b> You are given a story, which can be either a novel or a movie script, and a question. Answer the question as concisely as you can, using a single phrase if possible. Do not provide any explanation.</p> <p>Story: {context}</p> <p>Now, answer the question based on the story as concisely as you can, using a single phrase if possible. Do not provide any explanation.</p> <p>Question: {question}</p>
Qasper	<p><b>Task Template:</b> You are given a scientific article and a question. Answer the question as concisely as you can, using a single phrase or sentence if possible. If the question cannot be answered based on the information in the article, write "unanswerable". If the question is a yes/no question, answer "yes", "no", or "unanswerable". Do not provide any explanation.</p> <p>Article: {context}</p> <p>Answer the question based on the above article as concisely as you can, using a single phrase or sentence if possible. If the question cannot be answered based on the information in the article, write "unanswerable". If the question is a yes/no question, answer "yes", "no", or "unanswerable". Do not provide any explanation.</p> <p>Question: {question}</p>
MultifieldQA EN	<p><b>Task Template:</b> Read the following text and answer briefly.</p> <p>{context}</p> <p>Now, answer the following question based on the above text, only give me the answer and do not output any other words.</p> <p>Question: {question}</p>

Table 6: LongBench templates. Multi-Doc. QA Tasks.

HotpotQA	<p><b>Task Template:</b> Answer the question based on the given passages. Only give me the answer and do not output any other words.</p> <p>The following are given passages. {context}</p> <p>Answer the question based on the given passages. Only give me the answer and do not output any other words.</p> <p>Question: {question}</p>
2WikimQA	<p><b>Task Template:</b> Answer the question based on the given passages. Only give me the answer and do not output any other words.</p> <p>The following are given passages. {context}</p> <p>Answer the question based on the given passages. Only give me the answer and do not output any other words.</p> <p>Question: {question}</p>
Musique	<p><b>Task Template:</b> Answer the question based on the given passages. Only give me the answer and do not output any other words.</p> <p>The following are given passages. {context}</p> <p>Answer the question based on the given passages. Only give me the answer and do not output any other words.</p> <p>Question: {question}</p>

Table 7: LongBench templates. Summarization Tasks.

Gov Report	<p><b>Task Template:</b> You are given a report by a government agency. Write a one-page summary of the report.</p> <p>Report: {context}</p> <p>Now, write a one-page summary of the report.</p>
QMSum	<p><b>Task Template:</b> You are given a meeting transcript and a query containing a question or instruction. Answer the query in one or more sentences.</p> <p>Transcript: {context}</p> <p>Now, answer the query based on the above meeting transcript in one or more sentences.</p> <p>Query: {question}</p>
Multi News	<p><b>Task Template:</b> You are given several news passages. Write a one-page summary of all news.</p> <p>News: {context}</p> <p>Now, write a one-page summary of all the news.</p>

Table 8: LongBench templates. Few-shot Learning Tasks.

TREC	<p><b>Task Template:</b> Please determine the type of the question below. Here are some examples of questions.</p> <p>{context}</p> <p>{question}</p>
TriviaQA	<p><b>Task Template:</b> Answer the question based on the given passage. Only give me the answer and do not output any other words. The following are some examples.</p> <p>{context}</p> <p>{question}</p>
SAMSum	<p><b>Task Template:</b> Summarize the dialogue into a few short sentences. The following are some examples.</p> <p>{context}</p> <p>{question}</p>

Table 9: LongBench templates. Synthetic Tasks.

Passage Count	<p><b>Task Template:</b> There are some paragraphs below sourced from Wikipedia. Some of them may be duplicates. Please carefully read these paragraphs and determine how many unique paragraphs there are after removing duplicates. In other words, how many non-repeating paragraphs are there in total?</p> <p>{context}</p> <p>Please enter the final count of unique paragraphs after removing duplicates. The output format should only contain the number, such as 1, 2, 3, and so on.</p>
Passage Retrieval EN	<p><b>Task Template:</b> Here are 30 paragraphs from Wikipedia, along with an abstract. Please determine which paragraph the abstract is from.</p> <p>{context}</p> <p>The following is an abstract.</p> <p>{question}</p> <p>Please enter the number of the paragraph that the abstract is from. The answer format must be like "Paragraph 1", "Paragraph 2", etc.</p>

Table 10: LongBench templates. Code Tasks.

Lcc	<p><b>Task Template:</b> Please complete the code given below.</p> <p>{context}</p> <p>Next line of code:</p>
Repobench-P	<p><b>Task Template:</b> Please complete the code given below.</p> <p>{context}</p> <p>{question}</p> <p>Next line of code:</p>